ML Time Delay Estimation for 5G Links with DSSS Multi-Carrier Multipath MIMO Radio Access

Ahmed Masmoudi[1], Faouzi Bellili[1], Sofiène Affes[1], and Ali Ghrayeb[2]

[1]INRS-EMT, 800, de la Gauchetière Ouest, Bureau 6900, Montreal, Qc, H5A 1K6, Canada
[2]Texas A&M University at Qatar, Engineering Building, Education City, Doha, Qatar
Emails: {masmoudi, bellili, affes}@emt.inrs.ca, ali.ghrayeb@qatar.tamu.edu

***Abstract*—This paper presents two new implementations of the maximum likelihood (ML) time delay estimation (TDE) from multi-carrier (MC) Direct-Sequence Spread Spectrum (DSSS) in multipath MIMO transmissions that will characterize future 5G radio interface technologies (RITs). The first TDE, based on expectation maximization (EM), provides accurate estimates of the delays when a good initialisation of the parameters is available. The second TDE returns the global maximum of the *compressed* likelihood function (CLF) using the importance sampling (IS) technique without requiring any initialization. Interestingly, in the non-data-aided (NDA) case, temporal, spatial (transmit and receive), and frequency samples have the same impact on estimation accuracy and performance bound which depends on the product of these dimensions regardless of the channel correlation type. Furthermore, we cope with such channel correlations that arise in practice and, hence, become very challenging both in estimation and CRLB derivation in the data-aided (DA) case, but that have been so far overlooked in previous works.**

***Index Terms*—DSSS, 5G, TDE, post-correlation model (PCM), ML, CRLB, EM, importance sampling (IS), DA, NDA.**

I. Introduction

MC DSSS RITs are able to operate at high data rates with high bandwidth efficiency and are robust to adverse conditions of channel frequency selectivity [4, 5], more so when implemented in MIMO structures. Therefore, they have the potential to be adopted in future 5G high-density wireless networks. Yet, to ensure good performance, these systems require large time synchronization capabilities. In this work, we focus on the post correlation model (PCM) of the despread data which presents the signal in a manifold structure that has been massively studied in the area of array signal processing. To date, an implementation of root-MUSIC was initially presented in [6] to estimate the time delays. As a low-complexity subspace-based method, it relies on the maximization of the spectrum of the received signal to find its peak frequency components. The present work investigates the ML-based TDEs for MIMO MC-DSSS systems that avoid the computationally-prohibitive multidimensional grid-search approach using the PCM [5, 6]. Without lack of generality, we consider MC CDMA array receivers as a case of study.

We first develop an efficient iterative solution for the estimation of the delays using the EM concept. While this concept was previously leveraged to solve the problem of multiple time delays estimation [7], it has not been adapted to the context of MIMO MC-DSSS systems. Alternatively, when an initial guess is not available, we resort to the IS concept to find the global maximum of the CLF in a non-iterative way.

The contributions of this work cover MC DSSS with any antenna configuration. While the MC DSSS show-case considered herein, without lack of generality, is MC-DS-CDMA, all developments presented in the article remain valid for other single carrier (SC) or MC DSSS RITs such as cdma2000, WCDMA, IEEE 802.11b implemented standards, multitone-CDMA [8] and prospective 5G coded-domain NOMA [9].

In [1], we proposed an EM ML TDE for SIMO DS-CDMA transmissions with a straightforward extension to MC-DS-CDMA by applying the EM algorithm on each subcarrier separately and then averaging the resulting estimates from all subcarriers. Here, we propose 1) a more judicious implementation of the algorithm to MC-DS-CDMA by applying it only once over all subcarriers jointly, 2) we extend it to the DA case; and 3) from SIMO to MIMO transceivers. A basic version of the IS TDE was also presented in [2] for SIMO SC-DS-CDMA NDA only. Here we 4) consider the cases of

This work was made possible by NPRP grant NPRP 5-250-2-087 from the Qatar National Research Fund (a member of the Qatar Foundation). The statements made herein are solely the responsibility of the authors. Preliminary findings were disclosed in [1] and [2] before new major developments of this initial work have become confidential material of the above-mentioned 2013-2016 research project until completion. Most recent results of this project, disclosed herein and in an accepted journal version [3], have never been published nor presented previously in any conference venue.

DA, MC, and MIMO transmissions. We also 5) develop for the first time the most general closed-form CRLB expressions ever for MC DSSS transmissions with either SISO, SIMO, MISO, or MIMO transceiver structures with any diversity versus multiplexing pre-coding type, apply in both NDA and DA cases, and account for the impact of channel correlation in space, time, and frequency that arise in the DA case but that have been overlooked in previous works.

II. System Model

A. NDA MC Transmissions

We consider a SIMO MC-DS-CDMA communication system where the receiver is equipped with M receive antennas and a multipath channel consisting of P different paths. The received signals over each subcarrier are decorrelated with the spreading code and sampled at the chip rate T_c. Denoting the processing gain by $L = T/T_c$ where T is the symbol duration, the post-correlation data of the spatio-temporal observation during the n^{th} received symbol and the k^{th} subcarrier is [6]:

$$\boldsymbol{Z}_{k,n} = \boldsymbol{J}_{k,n}\boldsymbol{D}_k(\boldsymbol{\tau})^T s_{k,n} + \boldsymbol{N}_{k,n}, \boldsymbol{Z}_{k,n}^T, \tag{1}$$

where the unknown delays are gathered in the parameter vector $\boldsymbol{\tau} = [\tau_1, \ldots, \tau_P]^T$, $s_{k,n}$ is the unknown transmitted symbol, and $\boldsymbol{N}_{k,n}$ is the $M \times L$ post-correlation noise matrix. The p^{th} column of the matrix $\boldsymbol{D}_k(\boldsymbol{\tau})$ that gathers the time delay parameters, $\tau_1, \ldots, \tau_P$, is:

$$\mathbf{d}_{k,p} = e^{-j2\pi k\lambda\frac{\tau_p}{T_c M_c}}\Big[\rho_c(-\tau_p),\ \rho_c(T_c/k_s - \tau_p)e^{j2\pi k\frac{\lambda}{Lk_s}}, \ldots, \rho_c((Lk_s-1)T_c/k_s - \tau_p)e^{j2\pi k\frac{\lambda(Lk_s-1)}{Lk_s}}\Big]^T, \tag{2}$$

where M_c is the number of subcarriers, λ determines the frequency spacing between two adjacent subcarriers and k_s is the oversampling ratio [8]. We assume here that the time delays are the same across all subcarriers [8]. In (2), $\rho_c(.)$ is the correlation function of the spreading code. Unlike the SC case in [1], the received samples $\boldsymbol{Z}_{k,n}$ cannot be directly used as an input to the algorithms because of the presence of the exponential terms $e^{j2\pi k\frac{\lambda l}{Lk_s}}$ in the vector $\mathbf{d}_{k,p}$. Therefore, we introduce the intermediate variable $\dot{\boldsymbol{Z}}_{k,n}$ defined as:

$$\dot{\boldsymbol{Z}}_{k,n} = \boldsymbol{Z}_{k,n} \odot \left(\boldsymbol{a}\boldsymbol{1}_M^T\right) = s_{k,n}\boldsymbol{J}_{k,n}\dot{\boldsymbol{D}}_k^T(\boldsymbol{\tau}) + \dot{\boldsymbol{N}}_{k,n}, \tag{3}$$

where $\boldsymbol{a} \triangleq \left[1,\ e^{-j2\pi\frac{\lambda}{Lk_s}}, \ldots,\ e^{-j2\pi\frac{\lambda(Lk_s-1)}{Lk_s}}\right]^T$, $\odot$ stands for the element-wise product, and $\boldsymbol{1}_M \triangleq [1, \ldots, 1]^T$. The p^{th} column of $\dot{\boldsymbol{D}}_k(\boldsymbol{\tau})$ is given by:

$$\dot{\mathbf{d}}_{k,p} = \mathbf{d}_{k,p} \odot \boldsymbol{a} = e^{-j2\pi k\lambda\frac{\tau_p}{T_c M_c}}\big[\rho_c(-\tau_p), \rho_c(T_c/k_s - \tau_p), \ldots, \rho_c((Lk_s-1)T_c/k_s - \tau_p)\big]^T. \tag{4}$$

While the formulation in (3) seems to be adapted to our estimation process, the phase shift $e^{-j2\pi k\lambda\frac{\tau_p}{T_c M_c}}$ in each column of $\dot{\boldsymbol{D}}_k(\boldsymbol{\tau})$ prevents us from using directly the signal structure in (3). To overcome this problem, we note that $\dot{\boldsymbol{D}}_k(\boldsymbol{\tau})$ can be written as $\dot{\boldsymbol{D}}_k(\boldsymbol{\tau}) = \boldsymbol{D}(\boldsymbol{\tau})\boldsymbol{A}_k$ where $\boldsymbol{A}_k$ is a $P \times P$ diagonal matrix whose diagonal elements are $e^{-j2\pi k\lambda\frac{\tau_p}{T_c M_c}}$, $p = 1, \ldots, P$. Finally, to exploit gains from the frequency dimension, we gather all the transformed observations over the different subcarriers into the following compact representation:

$$\dot{\boldsymbol{Z}}_n \triangleq \left[\dot{\boldsymbol{Z}}_{1,n}^T,\ \dot{\boldsymbol{Z}}_{2,n}^T, \ldots,\ \dot{\boldsymbol{Z}}_{N_c,n}^T\right] = \boldsymbol{D}(\boldsymbol{\tau})\dot{\boldsymbol{J}}_n^T + \dot{\boldsymbol{N}}_n^T, \tag{5}$$

with $\dot{\boldsymbol{J}}_n^T \triangleq \left[\boldsymbol{A}_1\boldsymbol{J}_{1,n}^T, \ldots,\ \boldsymbol{A}_{N_c}\boldsymbol{J}_{N_c,n}^T\right]$ and $\dot{\boldsymbol{N}}_n^T \triangleq \left[\dot{\boldsymbol{N}}_{1,n}^T, \ldots,\ \dot{\boldsymbol{N}}_{N_c,n}^T\right]$. The main advantage of the formulation in (5) is the increase of the number of observations, proportionately to the number of subcarriers. By concatenating N observed symbols, we obtain:

$$\dot{\boldsymbol{Z}} \triangleq \left[\dot{\boldsymbol{Z}}_1,\ \dot{\boldsymbol{Z}}_2, \ldots,\ \dot{\boldsymbol{Z}}_N\right] = \boldsymbol{D}(\boldsymbol{\tau})\dot{\boldsymbol{J}}^T + \dot{\boldsymbol{N}}^T, \tag{6}$$

where $\dot{\boldsymbol{J}}^T \triangleq \left[\dot{\boldsymbol{J}}_1^T, \ldots,\ \dot{\boldsymbol{J}}_N^T\right]$ and $\dot{\boldsymbol{N}}^T \triangleq \left[\dot{\boldsymbol{N}}_1^T, \ldots,\ \dot{\boldsymbol{N}}_N^T\right]$. Before presenting the ML solutions, we perform a column-by-column fast Fourier transform (FFT) of $\dot{\boldsymbol{Z}}$ to obtain:

$$\dot{\boldsymbol{\mathcal{Z}}} = \boldsymbol{\mathcal{D}}(\boldsymbol{\tau})\dot{\boldsymbol{J}}^T + \dot{\boldsymbol{\mathcal{N}}}^T, \tag{7}$$

where $\dot{\boldsymbol{\mathcal{N}}}^T$ is the resulting transformed noise matrix and $\boldsymbol{\mathcal{D}}(\boldsymbol{\tau})$ depends only on the unknown delays as:

$$\boldsymbol{\mathcal{D}}(\boldsymbol{\tau}) = \left[\boldsymbol{d}(\tau_1),\ \boldsymbol{d}(\tau_2), \ldots,\ \boldsymbol{d}(\tau_P)\right], \tag{8}$$

where $\boldsymbol{d}(\tau_p) = \left[c_0,\ c_1 e^{-\frac{j2\pi\tau_p}{LT_c}}, \ldots,\ c_{L-1}e^{-\frac{j2\pi(L-1)\tau_p}{LT_c}}\right]^T$ depends on the p^{th} delay and $\{c_l\}_{l=0}^{L-1}$ are the FFT coefficients of the spreading code correlation function.

B. NDA MIMO Transmission

For MIMO transmission, we assume M_{Tx} co-located transmit antennas characterized each by its own spreading code and M_{Tx} sources s_k for $k = 1, \ldots, M_{\text{Tx}}$ that stem from any given mixture of other M_{Tx} sources s'_k for $k = 1, \ldots, M_{\text{Tx}}$ to translate pure transmit diversity, pure transmit multiplexing, or any combination thereof, then (7) also holds in the MIMO case:

$$\boldsymbol{\mathcal{Z}}_k = \boldsymbol{\mathcal{D}}(\boldsymbol{\tau})\boldsymbol{J}_k^T + \boldsymbol{\mathcal{N}}_k^T, \tag{9}$$

where $k = 1, \ldots, M_{\text{Tx}}$ stands for the transmit antenna index. For a more compact representation, we stack all the M_{Tx} matrices in (9) into one matrix $\boldsymbol{\mathcal{Z}}_{\text{MIMO}} \triangleq [\boldsymbol{\mathcal{Z}}_1, \ldots,\ \boldsymbol{\mathcal{Z}}_{M_{\text{Tx}}}]$.

III. The EM-Based ML TDE

We assume that the multipath fading coefficients, gathered in $\boldsymbol{J}$, are random variables with unknown diagonal covariance matrix $\boldsymbol{R}_{\boldsymbol{J}}$. In the following, $\boldsymbol{R}_{\boldsymbol{J}}$ is assumed to be the same for all receiving antennas and remains constant. We suppose that $\boldsymbol{\mathcal{Z}}_{\text{MIMO}}$ has independent columns, denoted $\mathcal{Z}_i$. Therefore, the log-likelihood function (LLF) parametrized by $\boldsymbol{\tau}$ and the covariance matrix $\boldsymbol{R_J}$ of the columns of $\boldsymbol{J}_n^T$, is:

$$\mathcal{L}(\boldsymbol{\tau}, \boldsymbol{R_J}) = -\ln\Big(\det\Big\{\boldsymbol{\mathcal{D}(\tau)} \boldsymbol{R_J} \boldsymbol{\mathcal{D}(\tau)}^H + \sigma^2 \boldsymbol{I}_L\Big\}\Big) - \frac{1}{MNN_cM_{\text{Tx}}} \sum_{i=1}^{MNN_cM_{\text{Tx}}} \boldsymbol{\mathcal{Z}}_i^H \Big(\boldsymbol{\mathcal{D}(\tau)} \boldsymbol{R_J} \boldsymbol{\mathcal{D}(\tau)}^H + \sigma^2 \boldsymbol{I}_L\Big)^{-1} \boldsymbol{\mathcal{Z}}_i \quad (10)$$

where $\det\{.\}$ returns the determinant of a square matrix and $\boldsymbol{I}_L$ is the $L \times L$ identity matrix. Rewriting the LLF in (10) in a more compact form, we obtain:

$$\mathcal{L}(\boldsymbol{\tau}, \boldsymbol{R_J}) = -\ln\big(\det\{\boldsymbol{R}_{\boldsymbol{\mathcal{Z}}}\}\big) - \text{tr}\Big\{\boldsymbol{R}_{\boldsymbol{\mathcal{Z}}}^{-1} \widehat{\boldsymbol{R}}_{\boldsymbol{\mathcal{Z}}}\Big\}, \quad (11)$$

with $\widehat{\boldsymbol{R}}_{\boldsymbol{\mathcal{Z}}} = \frac{1}{N_{\text{total}}} \sum_{i=1}^{N_{\text{total}}} \boldsymbol{\mathcal{Z}}_i \boldsymbol{\mathcal{Z}}_i^H$ being an estimate of the actual covariance matrix $\boldsymbol{R}_{\boldsymbol{\mathcal{Z}}}$ and $N_{\text{total}} = MNN_cM_{\text{Tx}}$. Note here that the LLF, $\mathcal{L}(\boldsymbol{\tau}, \boldsymbol{R_J})$, depends on the vector of interest, $\boldsymbol{\tau}$, and the unknown covariance matrix $\boldsymbol{R_J}$. The goal is therefore to jointly maximize $\mathcal{L}(\boldsymbol{\tau}, \boldsymbol{R_J})$ with respect to $\boldsymbol{\tau}$ and $\boldsymbol{R_J}$.

Clearly, we cannot directly maximize the LLF in (11). Thus, we resort to the iterative EM concept [7]. The purpose is to decompose the observation vectors $\{\boldsymbol{\mathcal{Z}}_i\}_{i=1}^{N_{\text{total}}}$ into P complete-data from which the P delays are estimated separately. We first define the complete data:

$$\boldsymbol{z}^{(p)}(i) = \boldsymbol{J}^T(i,p)\boldsymbol{d}(\tau_p) + \boldsymbol{n}^{(p)}(i), \quad p = 1, \ldots, P, \; i = 1, \ldots, N_{\text{total}}, \quad (12)$$

where $\boldsymbol{z}^{(p)}(i)$ can be seen as the i^{th} spatio-temporal snapshot from the p^{th} path $\big($i.e., $\boldsymbol{\mathcal{Z}_i} = \sum_{p=1}^{P} \boldsymbol{z}^{(p)}(i)\big)$ and $\boldsymbol{n}^{(p)}(i)$ is an arbitrary decomposition of the noise. From (12), the covariance of $\boldsymbol{z}^{(p)}(i)$, $\mathbb{E}\big\{\boldsymbol{z}^{(p)}(i)\boldsymbol{z}^{(p)}(i)^H\big\}$ is given by:

$$\boldsymbol{R}_{\boldsymbol{z}^{(p)}} = \varepsilon_p^2 \boldsymbol{d}(\tau_p)\boldsymbol{d}(\tau_p)^H + \frac{\sigma^2}{P}\boldsymbol{I}_L, \quad (13)$$

with $\{\varepsilon_p^2\}_{p=1}^P$ being the diagonal elements of $\boldsymbol{R_J}$.

In the E-step, we compute the conditional expectations of the sample covariance matrices $\{\widehat{\boldsymbol{R}}_{\boldsymbol{z}^{(p)}}\}_{p=1}^P$ of the complete data, defined as $\widehat{\boldsymbol{R}}_{\boldsymbol{z}^{(p)}} = \frac{1}{N_{\text{total}}} \sum_{i=1}^{N_{\text{total}}} \boldsymbol{z}^{(p)}(i)\left(\boldsymbol{z}^{(p)}(i)\right)^H$. Given $\widehat{\boldsymbol{R}}_{\boldsymbol{\mathcal{Z}}}$, $\boldsymbol{R}_{\boldsymbol{J}}^{\{q-1\}}$ and $\boldsymbol{\tau}^{\{q-1\}}$ $\big($the estimates of $\boldsymbol{R_J}$ and $\boldsymbol{\tau}$ at iteration $(q-1)\big)$, the expectation of $\widehat{\boldsymbol{R}}_{\boldsymbol{z}^{(p)}}$ can be evaluated as follows:

$$\begin{aligned}\widehat{\boldsymbol{R}}_{\boldsymbol{z}^{(p)}}^{\{q\}} &= \mathbb{E}\Big\{\widehat{\boldsymbol{R}}_{\boldsymbol{z}^{(p)}} \Big| \widehat{\boldsymbol{R}}_{\boldsymbol{\mathcal{Z}}}; \boldsymbol{R}_{\boldsymbol{J}}^{\{q-1\}}; \boldsymbol{\tau}^{\{q-1\}}\Big\} \\ &= \boldsymbol{R}_{\boldsymbol{z}^{(p)}}^{\{q\}} \left(\boldsymbol{R}_{\boldsymbol{\mathcal{Z}}}^{\{q\}}\right)^{-1} \widehat{\boldsymbol{R}}_{\boldsymbol{\mathcal{Z}}} \left(\boldsymbol{R}_{\boldsymbol{\mathcal{Z}}}^{\{q\}}\right)^{-1} \boldsymbol{R}_{\boldsymbol{z}^{(p)}}^{\{q\}} + \boldsymbol{R}_{\boldsymbol{z}^{(p)}}^{\{q\}} \\ &\quad - \boldsymbol{R}_{\boldsymbol{z}^{(p)}}^{\{q\}} \left(\boldsymbol{R}_{\boldsymbol{\mathcal{Z}}}^{\{q\}}\right)^{-1} \boldsymbol{R}_{\boldsymbol{z}^{(p)}}^{\{q\}}, \quad (14)\end{aligned}$$

where the matrices $\boldsymbol{R}_{\boldsymbol{z}^{(p)}}^{\{q\}}$ are computed at the q^{th} iteration from the estimates $\tau_p^{\{q-1\}}$ and $\varepsilon_p^{2\,\{q-1\}}$ already computed at iteration $q-1$. Now, turning to the estimation of $\boldsymbol{R}_{\boldsymbol{\mathcal{Z}}}^{\{q\}}$, the procedure is different from the one used in previous EM algorithms in [7] and [10] where the covariance matrix of the received signal is simply diagonal, contrarily to the problem at hand. Therefore, we resort here to another approach to estimate the covariance matrix $\boldsymbol{R}_{\boldsymbol{\mathcal{Z}}}^{\{q\}}$ based on the method of estimating Toeplitz-structured matrices detailed in [3].

During the M-step of the EM algorithm, we aim at maximizing the LLF of the complete-data with respect to the parameters of interest $\{\tau_i\}_{i=1}^P$. It is the same objective function given in (10), with the true expectation of the complete data being replaced by the conditional expectation of $\boldsymbol{z}^{(p)}(i)$; in other words $\boldsymbol{R}_{\boldsymbol{\mathcal{Z}}}$ is substituted by $\boldsymbol{R}_{\boldsymbol{z}^{(p)}}$ and $\widehat{\boldsymbol{R}}_{\boldsymbol{\mathcal{Z}}}$ by $\widehat{\boldsymbol{R}}_{\boldsymbol{z}^{(p)}}^{\{q\}}$. Thus, we obtain the LLF of the complete-data, $\mathcal{L}_p(\tau_p, \boldsymbol{R}_{\boldsymbol{z}^{(p)}})$, as follows:

$$\mathcal{L}_p(\tau_p, \boldsymbol{R}_{\boldsymbol{z}^{(p)}}) = -\ln\left(\det\{\boldsymbol{R}_{\boldsymbol{z}^{(p)}}\}\right) - \text{tr}\Big\{\widehat{\boldsymbol{R}}_{\boldsymbol{z}^{(p)}}^{\{q\}} \boldsymbol{R}_{\boldsymbol{z}^{(p)}}^{-1}\Big\}.$$

Then, at iteration q, the estimates $\widehat{\tau}_p^{\{q\}}$ and $\widehat{\boldsymbol{R}}_{\boldsymbol{z}^{(p)}}^{\{q\}}$ are those which jointly maximize $\mathcal{L}_p(\tau_p, \boldsymbol{R}_{\boldsymbol{z}^{(p)}})$. Using the eigen-decomposition[1] of $\boldsymbol{R}_{\boldsymbol{z}^{(p)}}$, the LLF of the complete-data can be expressed as:

$$\mathcal{L}_p(\tau_p, \boldsymbol{R}_{\boldsymbol{z}^{(p)}}) = -\ln\left(\varepsilon_p^2 + \frac{\sigma^2}{P}\right) - (M-1)\ln\left(\frac{\sigma^2}{P}\right) \left(\frac{1}{\varepsilon_p^2 + \frac{\sigma^2}{P}} - \frac{P}{\sigma^2}\right) \boldsymbol{d}(\tau_p)^H \widehat{\boldsymbol{R}}_{\boldsymbol{z}^{(p)}}^{\{q\}} \boldsymbol{d}(\tau_p) - \frac{P}{\sigma^2}\text{tr}\Big\{\widehat{\boldsymbol{R}}_{\boldsymbol{z}^{(p)}}^{\{q\}}\Big\}, \quad (15)$$

which emphasizes the dependence of $\mathcal{L}_p(\tau_p, \boldsymbol{R}_{\boldsymbol{z}^{(p)}})$ on τ_p and ε_p^2. The closed-form expression of its maximum with respect to ε_p^2, for a given $\tau_p^{\{q\}}$, is:

$$\varepsilon_p^{2\,\{q\}} = \boldsymbol{d}\big(\tau_p^{\{q\}}\big)^H \widehat{\boldsymbol{R}}_{\boldsymbol{z}^{(p)}}^{\{q\}} \boldsymbol{d}\big(\tau_p^{\{q\}}\big) - \frac{\sigma^2}{P}. \quad (16)$$

Now, plugging (16) in (15) yields the following one-dimensional maximization problem:

$$\begin{aligned}\tau_p^{\{q\}} = \arg\max_{\tau_p} \Big\{ &-\ln\Big(\boldsymbol{d}(\tau_p)^H \widehat{\boldsymbol{R}}_{\boldsymbol{z}^{(p)}}^{\{q\}} \boldsymbol{d}(\tau_p)\Big) \\ &+ \frac{P}{\sigma^2} \boldsymbol{d}(\tau_p)^H \widehat{\boldsymbol{R}}_{\boldsymbol{z}^{(p)}}^{\{q\}} \boldsymbol{d}(\tau_p)\Big\}, \quad (17)\end{aligned}$$

or simply by maximizing $\boldsymbol{d}(\tau_p)^H \widehat{\boldsymbol{R}}_{\boldsymbol{z}^{(p)}}^{\{q\}} \boldsymbol{d}(\tau_p)$.

IV. The IS ML TDE

As mentioned earlier, a direct maximization of the LLF in (10) imposes joint maximization over $\boldsymbol{\tau}$ and $\boldsymbol{R_J}$. Therefore, we first maximize the LLF with respect to the matrix $\boldsymbol{R_J}$, for a fixed vector $\boldsymbol{\tau}$, thereby leading to:

$$\widehat{\boldsymbol{R}}_{\boldsymbol{J}}^{\text{ML}} = \big[\boldsymbol{\mathcal{D}(\tau)}^H \boldsymbol{\mathcal{D}(\tau)}\big]^{-1} \boldsymbol{\mathcal{D}(\tau)}^H \widehat{\boldsymbol{R}}_{\mathcal{Z}} \boldsymbol{\mathcal{D}(\tau)} \times \big[\boldsymbol{\mathcal{D}(\tau)}^H \boldsymbol{\mathcal{D}(\tau)}\big]^{-1} - \sigma^2 \big[\boldsymbol{\mathcal{D}(\tau)}^H \boldsymbol{\mathcal{D}(\tau)}\big]^{-1}. \quad (18)$$

Then, using $\widehat{\boldsymbol{R}}_{\boldsymbol{J}}^{\text{ML}}$ back into (10) yields the CLF:

$$\mathcal{L}_c(\boldsymbol{\tau}) = \frac{1}{\sigma^2}\text{tr}\Big\{\boldsymbol{\Pi}\widehat{\boldsymbol{R}}_{\boldsymbol{\mathcal{Z}}}\Big\} - \ln\Big(\det\Big\{\boldsymbol{\Pi}\widehat{\boldsymbol{R}}_{\boldsymbol{\mathcal{Z}}}\boldsymbol{\Pi} + \sigma^2\boldsymbol{\Pi}^{\perp}\Big\}\Big), \quad (19)$$

[1] The matrix $\varepsilon_p^2 \boldsymbol{d}(\tau_p)\boldsymbol{d}(\tau_p)^H$ is of rank one with only one nonzero eigenvalue, therefore the eigen-decomposition of $\boldsymbol{R}_{\boldsymbol{z}^{(p)}}$ can be easily performed.

where $\mathbf{\Pi} = \boldsymbol{\mathcal{D}}(\boldsymbol{\tau}) \left[\boldsymbol{\mathcal{D}}(\boldsymbol{\tau})^H \boldsymbol{\mathcal{D}}(\boldsymbol{\tau})\right]^{-1} \boldsymbol{\mathcal{D}}(\boldsymbol{\tau})^H$. Now, the ML estimates of the time delays are obtained by maximizing the CLF $\mathcal{L}_c(\boldsymbol{\tau})$ with respect to $\boldsymbol{\tau}$. Here, we introduce a non-iterative implementation of the ML criterion. We resort to the global maximization theorem of Pincus [11] in order to find the global maximum of the underlying multi-dimensional CLF. In fact, according to [11], the global maximum, $\widehat{\boldsymbol{\tau}} \triangleq [\widehat{\tau}_1, \ldots, \widehat{\tau}_P]^T$, of $\mathcal{L}_c(\boldsymbol{\tau})$ with respect to $\boldsymbol{\tau}$ is $\widehat{\boldsymbol{\tau}} = \frac{1}{R}\sum_{r=1}^{R} \boldsymbol{\tau}_r$, where $\{\boldsymbol{\tau}_r\}_{r=1}^{R}$ are R realizations of $\boldsymbol{\tau}$, distributed according to the pseudo-probability density function (PDF) $\mathcal{L}'_{c,\rho}(.)$:

$$\mathcal{L}'_{c,\rho}(\boldsymbol{\tau}) = \frac{\exp\{\rho \mathcal{L}_c(\boldsymbol{\tau})\}}{\int_J \ldots \int_J \exp\{\rho \mathcal{L}_c(\boldsymbol{\tau})\}\, d\boldsymbol{\tau}}, \tag{20}$$

with $J = [0, T]$ being the interval in which the delays are confined. The pseudo-PDF $\mathcal{L}'_{c,\rho}(.)$ is formulated using the actual CLF in (19), which is a P-dimensional function; making the generation of the vector $\boldsymbol{\tau}$ very difficult. Therefore, it is of interest to find an alternative pseudo-PDF to generate the realizations. To do so, we resort to the IS concept by generating realizations using another distribution which is simpler than the actual one. The IS approach is based on the following observation:

$$\frac{1}{R}\sum_{r=1}^{R} \boldsymbol{\tau}_r \approx \frac{1}{R}\sum_{r=1}^{R} \boldsymbol{\tau}_r \frac{\mathcal{L}'_{c,\rho}(\boldsymbol{\tau})}{g'(\boldsymbol{\tau})} \tag{21}$$

in which the realizations $\{\boldsymbol{\tau}_r\}_{r=1}^{R}$ are now generated according to another pseudo-PDF $g'(.)$, called *importance function* (IF). Yet, we should carefully choose $g'(.)$. In fact, the approximation in (21) depends on the similarity between the shapes of $\mathcal{L}'_{c,\rho}(.)$ and $g'(.)$. Ideally, the global maxima of $\mathcal{L}'_{c,\rho}(.)$ and $g'(.)$ are the same. Still, $\mathcal{L}'_{c,\rho}(.)$ is a complicated function of $\boldsymbol{\tau}$ and $g'(.)$ must be as simple as possible to easily generate the required realizations. The IF is selected as [3]:

$$g'_{\rho_1}(\boldsymbol{\tau}) = \frac{\prod_{p=1}^{P} \exp\{\rho_1 I(\tau_p)\}}{\left(\int_J \exp\{\rho_1 I(\tau)\}\, d\tau\right)^P}, \tag{22}$$

where:

$$I(\tau) = \frac{1}{N_{\text{total}}\sigma^2} \sum_{k=1}^{N_{\text{total}}} \left| \sum_{l=1}^{L} c_{l-1} \exp\left\{-\frac{j2\pi(l-1)\tau}{L}\right\} [\boldsymbol{\mathcal{Z}}]_{k,l} \right|, \tag{23}$$

can be evaluated using the FFT of $[\boldsymbol{\mathcal{Z}}]_{k,l}$. The IF in (22) is the product of P elementary functions, each one depends on the single delay of a given single path. Here, we succeeded in finding a normalized IF for which the different delays are separable and identically distributed according to the same pseudo-PDF $p(.)$ given by:

$$p(\tau) = \frac{\exp\{\rho_1 I(\tau)\}}{\int_J \exp\{\rho_1 I(\tau)\}\, d\tau}. \tag{24}$$

V. The CRLB

In this section, we provide a closed-form expression for the CRLB which will be used as a benchmark against which we gauge the performance of the TDEs. The CRLB in the MIMO MC DSSS NDA is given by [3]:

$$\begin{aligned}\text{CRLB} &= \frac{\sigma^2}{2MNN_cM_{\text{Tx}}} \times \\ &\left[\Re\left\{\left(\boldsymbol{U}^H \mathbf{\Pi}^{\perp} \boldsymbol{U}\right) \odot \left(\boldsymbol{R_j} \boldsymbol{\mathcal{D}}(\boldsymbol{\tau})^H \boldsymbol{R}_{\dot{\boldsymbol{\mathcal{Z}}}}^{-1} \boldsymbol{\mathcal{D}}(\boldsymbol{\tau}) \boldsymbol{R_j}\right)^T\right\}\right]^{-1} \\ &= \frac{1}{N_{\text{total}}}\, \text{CRLB}_0,\end{aligned} \tag{25}$$

where $\boldsymbol{R_j}$ and $\boldsymbol{R}_{\dot{\boldsymbol{\mathcal{Z}}}}$ are the covariance matrices of $\dot{\boldsymbol{J}}$ and $\dot{\boldsymbol{\mathcal{Z}}}$, respectively, $\mathbf{\Pi}^{\perp} = \boldsymbol{I}_L - \mathbf{\Pi}$, and $\boldsymbol{U}$ is defined as:

$$\boldsymbol{U} \triangleq [\boldsymbol{u}_1, \ldots,\ \boldsymbol{u}_P] = \left[\frac{\partial \boldsymbol{d}(\tau_1)}{\partial \tau_1}, \ldots,\ \frac{\partial \boldsymbol{d}(\tau_P)}{\partial \tau_P}\right], \tag{26}$$

and CRLB_0 is the CRLB when $M_{\text{Tx}} = M = N = N_c = 1$. As a consequence, the TDE in MIMO MC-DS-CDMA systems merges time, space and frequency dimensions whereby all samples have the same impact on estimation performance regardless of amount in each dimension.

VI. Extension to the DA Case

In the NDA case, the columns of the observation matrix are uncorrelated due to the presence of uncorrelated transmitted symbols. While in the DA case, these columns become correlated due to time, space, and frequency channel correlations. These correlations have to be properly incorporation in the estimation process and in the CRLB derivation. In the following, we cope with these correlations by following a new approach that is completely different from previous works. The extension to MIMO with any diversity-multiplexing configuration can be obtained using the same lines as above.

A. The ML TDEs

The model in (1) can be used to obtain an estimate $\widehat{\boldsymbol{H}}_{k,n}$ of $\boldsymbol{H}_{k,n} = \boldsymbol{J}_{k,n}\boldsymbol{D}^T(\boldsymbol{\tau})$ [8]. Then, taking into account the estimation error, $\widehat{\boldsymbol{H}}_{k,n}$ is written as:

$$\widehat{\boldsymbol{H}}_{k,n}^T = \boldsymbol{D}(\boldsymbol{\tau})\boldsymbol{J}_{k,n}^T + \boldsymbol{E}_{k,n}^T, \tag{27}$$

where $\boldsymbol{E}_{k,n}^T$ is the channel estimation error matrix. In general, the power of $\boldsymbol{E}_{k,n}$ is lower than the power of $\boldsymbol{N}_{k,n}$ due to the SNR gain stemming from channel identification [12]. Note here that the matrix $\boldsymbol{J}_{k,n}$ no longer contains the transmitted symbols $s_{k,n}$ thereby resulting in a DA scenario.

In the NDA case, the columns of the observation matrix are uncorrelated due to the presence of uncorrelated transmitted symbols. However, when the channel-coefficients matrix estimate $\widehat{\boldsymbol{H}} \triangleq \left[\widehat{\boldsymbol{H}}_{1,1}^T, \ldots, \widehat{\boldsymbol{H}}_{N_c,1}^T, \ldots,\ \widehat{\boldsymbol{H}}_{1,N}^T, \ldots, \widehat{\boldsymbol{H}}_{N_c,N}^T\right]$ is directly used in the estimation process, these symbols are no longer present and we are actually estimating the delays from the inherently correlated columns of $\widehat{\boldsymbol{H}}$. Therefore, we slightly modify the signal model to keep the two algorithms valid. First, we perform the FFT of $\widehat{\boldsymbol{H}}_{k,n}^T$ to obtain:

$$\begin{aligned}\widehat{\boldsymbol{\mathcal{H}}}_{k,n} &= \boldsymbol{\mathcal{D}}(\boldsymbol{\tau})\dot{\boldsymbol{J}}_{k,n}^T + \boldsymbol{\mathcal{E}}_{k,n} \\ &= \boldsymbol{\mathcal{D}}(\boldsymbol{\tau})\left[\boldsymbol{g}_{k,n}(1), \ldots, \ \boldsymbol{g}_{k,n}(M)\right] + \boldsymbol{\mathcal{E}}_{k,n}. \quad (28)\end{aligned}$$

Then, we stack the channel coefficients in the matrix $\widehat{\boldsymbol{\mathcal{H}}}$:

$$\widehat{\boldsymbol{\mathcal{H}}} = \overline{\boldsymbol{\mathcal{D}}}(\boldsymbol{\tau})\left[\boldsymbol{g}(1), \ \boldsymbol{g}(2), \ldots, \ \boldsymbol{g}(M)\right] + \boldsymbol{\mathcal{E}}, \quad (29)$$

with $\overline{\boldsymbol{\mathcal{D}}}(\boldsymbol{\tau}) = \boldsymbol{I}_N \otimes \boldsymbol{I}_{N_c} \otimes \boldsymbol{\mathcal{D}}(\boldsymbol{\tau})$ where the operator $\otimes$ stands for the Kronecker product and $\boldsymbol{g}(m) \triangleq \left[\boldsymbol{g}_{1,1}^T(m), \ldots, \ \boldsymbol{g}_{N_c,1}^T(m), \ \boldsymbol{g}_{1,2}^T(m), \ldots, \ \boldsymbol{g}_{N_c,2}^T(m), \ldots, \ \boldsymbol{g}_{1,N}^T(m), \ldots, \ \boldsymbol{g}_{N_c,N}^T(m)\right]^T$. Here, the two algorithms can be applied to $\widehat{\boldsymbol{\mathcal{H}}}$ in (29) instead[2] of $\dot{\boldsymbol{Z}}$ in (7).

B. The CRLB

Denote the autocorrelation of the channel transfer function as $\phi(\Delta f, \Delta t)$. Here, we consider uncorrelated scattering where this autocorrelation across subcarriers depends only on the frequency difference, Δf [3]. The covariance matrix of $\boldsymbol{g}(m)$ is hence $\boldsymbol{R}_{\boldsymbol{g}} = \boldsymbol{\Phi} \otimes \boldsymbol{R}_{\boldsymbol{J}}$ where the elements of $\boldsymbol{\Phi}$ are function of $\phi(\Delta f, \Delta t)$. Injecting $\boldsymbol{R}_{\boldsymbol{g}}$ and $\overline{\boldsymbol{\mathcal{D}}}(\boldsymbol{\tau})$ in (25), the CRLB can be written in the following alternative form:

$$\left[\mathrm{CRLB}^{-1}(\boldsymbol{\tau})\right]_{i,j} = \tfrac{2M}{\sigma^2}\Re\Big\{\mathrm{tr}\Big\{\boldsymbol{I}_N \otimes \boldsymbol{I}_{N_c} \otimes \Big(\boldsymbol{\mathcal{D}}_j^H(\boldsymbol{\tau})\boldsymbol{\Pi}^{\perp}\boldsymbol{\mathcal{D}}_i(\boldsymbol{\tau})\Big) \Big(\boldsymbol{R}_{\boldsymbol{g}}\overline{\boldsymbol{\mathcal{D}}}^H(\boldsymbol{\tau})\boldsymbol{R}_{\boldsymbol{\mathcal{H}}}^{-1}\overline{\boldsymbol{\mathcal{D}}}(\boldsymbol{\tau})\boldsymbol{R}_{\boldsymbol{g}}\Big)^T\Big\}\Big\}, \quad (30)$$

where $\boldsymbol{R}_{\boldsymbol{\mathcal{H}}}$ is the covariance of $\boldsymbol{\mathcal{H}}$ and $\overline{\boldsymbol{\mathcal{D}}}_i(\boldsymbol{\tau})$ and $\boldsymbol{\mathcal{D}}_i(\boldsymbol{\tau})$ are the derivatives of $\overline{\boldsymbol{\mathcal{D}}}(\boldsymbol{\tau})$ and $\boldsymbol{\mathcal{D}}(\boldsymbol{\tau})$ with respect to $\boldsymbol{\tau}_i$, respectively. If we denote by $\boldsymbol{B}_k$ the k^{th} $(P \times P)$ diagonal block of $\left(\boldsymbol{R}_{\boldsymbol{g}}\overline{\boldsymbol{\mathcal{D}}}^H\boldsymbol{R}_{\boldsymbol{\mathcal{H}}}^{-1}\overline{\boldsymbol{\mathcal{D}}}\boldsymbol{R}_{\boldsymbol{g}}\right)^T$, we obtain:

$$\left[\mathrm{CRLB}^{-1}(\boldsymbol{\tau})\right]_{i,j} = \tfrac{2M}{\sigma^2}\Re\left\{\sum_{k=1}^{NN_c}\left(\boldsymbol{u}_j^H\boldsymbol{\Pi}^{\perp}\boldsymbol{u}_i\right)\left[\boldsymbol{B}_k\right]_{i,j}\right\}. \quad (31)$$

Since $\boldsymbol{B}_k = \boldsymbol{B}$ when the second-order statistics of the P paths are the same, we obtain $\mathrm{CRLB}(\boldsymbol{\tau}) = \frac{1}{MNN_c}\mathrm{CRLB}_1(\boldsymbol{\tau})$, where $\mathrm{CRLB}_1(\boldsymbol{\tau}) = \Re\left\{\left(\boldsymbol{U}^H\boldsymbol{\Pi}^{\perp}\boldsymbol{U}\right) \odot \boldsymbol{B}\right\}$.

VII. Simulation Results

We consider a multipath Rayleigh-fading channel with $f_D T = 0.01$ and 3 equal-power paths in a challenging scenario of closely-spaced delays where $\boldsymbol{\tau} = [0.12\,T, \ 0.15\,T, \ 0.18\,T]$. We gauge the performance of the two proposed ML estimators against the root-MUSIC algorithm and the newly derived CRLBs. The initial values for the EM TDE are selected as random variables, centered at the true delays with variance $(0.05\,T)^2$. The processing gain is set to $L = 64$. For the IS-based technique, we set $\rho = 20$, $\rho_1 = 10$ and $R = 100$. The number of transmit antennas is $M_{\mathrm{Tx}} = 1$. The SNR is defined in the DA and NDA cases with respect to the powers of the channel estimation error and additive noise, respectively.

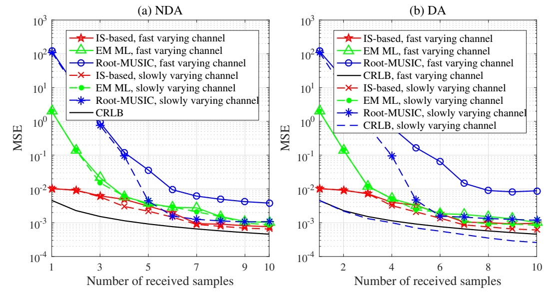

Fig. 1. MSE vs. the number of symbols N with $M = 1$ antenna, $N_c = 1$ subcarrier, and SNR $= 10$ dB for fast- ($f_D T = 0.01$) and slowly-varying ($f_D T = 10^{-4}$) channels in the (a): NDA and (b): DA cases.

The EM and root-MUSIC algorithms rely on an estimate of the received signal's covariance matrix from the columns of the matrix $\boldsymbol{\mathcal{Z}}$. The accuracy of this estimate depends on the number of temporal, spatial, and frequency snapshots. Therefore, we assess in Figs. 1 to 3 the performance of all these algorithms where one of the three dimensions is changed and set the others to 1. We also fix the SNR to 10 dB. Clearly, root-MUSIC and EM ML are sensitive to the number of snapshots and their performance degrades considerably over short data records due to the poor estimate of the covariance matrix $\boldsymbol{R}_{\boldsymbol{\mathcal{Z}}}$. On the other hand, the IS-based algorithm still provides good estimates with relatively few data snapshots. To assess the impact of channel time variations or correlation on performance, we now consider both the NDA and DA cases. We plot in Fig. 1 the MSE versus the number of received symbols N. For the fast varying channel, the three estimators exhibit almost the same performance for $N > 5$. For small numbers of snapshots, the new ML-based methods perform better than root-MUSIC and the advantage of the IS-based estimator becomes even more prominent in the single-snapshot case, and therefore suitable for real time applications. In the NDA case, there is almost no-dependency on the channel time variations or correlation. In the DA case, when using the channel matrix estimate, the ML-based methods still perform well, whereas root-MUSIC saturates at $N = 8$ for slowly time varying channels.

To investigate the impact of spatial correlation, we assess in Fig. 2 the estimation performance when the two adjacent antennas are correlated with correlation factors equal to 0.3 and 0.9. We plot the MSE versus M from

[2]For the MIMO case we substitute $\overline{\boldsymbol{\mathcal{D}}}$ by $\boldsymbol{I}_{M_{\mathrm{Tx}}} \otimes \boldsymbol{I}_N \otimes \boldsymbol{I}_{N_c} \otimes \boldsymbol{\mathcal{D}}$ and increase $\boldsymbol{g}(m)$ to include all the channel coefficients from the M_{Tx} antennas.

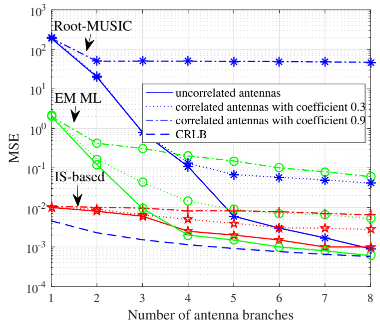

Fig. 2. MSE vs. the number of antennas M with $N = 1$ symbol, $N_c = 1$ subcarrier, and SNR $= 10$ dB.

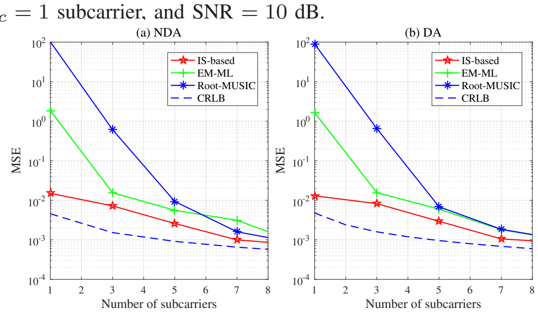

Fig. 3. MSE vs. the number of subcarriers N_c with $M = 1$ antenna, and $N = 1$ symbol, and SNR $= 10$ dB in the (a): NDA and (b): DA cases.

1 to 8 with $N = N_c = 1$. When the antennas are strongly correlated, increasing M does not bring much improvements.

In Fig. 3, we plot the MSE versus the number of subcarriers N_c at SNR $= 10$ dB in both the NDA and DA cases. We fix $M = N = 1$ to isolate the impact of the number of subcarriers N_c. As N_c increases, the estimation performance improves, then saturates at large values of N_c due to the increase of inter-carrier interference with N_c stemming from the loss of orthogonality between subcarriers in a multipath environment [8]. Also, the similarity between Figs. 1, 2, and 3 corroborates the fact that the space, time, and frequency dimensions have the same impact on the estimation performance.

VIII. Conclusion

In this paper, we developed two new ML TDEs and derived the corresponding CRLBs in closed-form for MC DSSS RITs with MIMO transceivers in both the NDA and DA cases. The first TDE relies on the iterative EM with a substantially reduced computational cost by transforming the multidimensional grid-search into parallel searches over one-dimensional spaces. The second ML TDE relies on Pincus' global maximization theorem and the IS concept to find the global maximum of the CLF. The IS TDE splits the CLF into separable one-dimensional functions of the delays. Only the IS TDE is able to deliver estimates from very short data records. In the NDA case, we revealed, both analytically and by simulations, that the space, time, and frequency dimensions interchangeably have exactly the same impact on estimation performance. Besides, we properly coped with such channel correlations that do arise in practice and, hence, become very challenging both in estimation and CRLB derivation in the DA case, but that have been so far overlooked in previous works.

References

[1] A. Masmoudi, F. Bellili, and S. Affes, "Time delays estimation from DS-CDMA multipath transmissions using expectation maximization," *Proc. of IEEE VTC'2012-Fall*, Quebec, Canada, Sep. 3-6, 2012.

[2] A. Masmoudi, F. Bellili, and S. Affes, "Maximum likelihood time delay estimation for direct-spread CDMA multipath transmissions using importance sampling," *Proc. ASILOMAR Signals, Syst., Comput.* Pacific Grove, USA, Nov. 6-9, 2011.

[3] A. Masmoudi, F. Bellili, S. Affes, and A. Ghrayeb, "Maximum Likelihood Time Delay Estimation from Single-and Multi-Carrier DSSS Multipath MIMO Transmissions for Future 5G Networks," *IEEE Trans. Wireless Comm.*, vol. 16, no. 128, pp. 4851-4865, Aug. 2017.

[4] I. Shakya, F. Ali, and E. Stipidis, "Robust joint resource allocation for OFDMA-CDMA spectrum refarming system," *IEEE Trans. on Comm.*, vol. 64, no. 3, pp. 1291-1302, Jan. 2016.

[5] K. Cheikhrouhou, S. Affes, and P. Mermelstein, "Impact of synchronization on performance of enhanced array-receivers in wideband CDMA networks," *IEEE J. Select. Areas in Comm.*, vol. 19, no. 12, pp. 2462-2476, Dec. 2001.

[6] S. Affes and P. Mermelstein, "A new receiver structure for asynchronous CDMA: STAR–the spatio-temporal array-receiver," *IEEE J. Select. Areas in Comm.*, vol. 16, no. 8, pp. 1411-1422, Oct. 1998.

[7] M. Feder and E. Weinstein, "Parameter estimation of superimposed signals using the EM algorithm," *IEEE Trans. Acoust., Speech, Sign. Process.*, vol. 36, pp. 477-489, Apr. 1988.

[8] B. Smida, S. Affes, L. Jun, and P. Mermelstein, "A spectrum-efficient multicarrier CDMA array-receiver with diversity-based enhanced time and frequency synchronization," *IEEE Trans. Wireless Commun.*, vol. 6, no. 6, pp. 2315-2327, June 2007.

[9] Q. Sun, S. Wang, S. Han, and I L. Chih, "Unified framework towards flexible multiple access schemes for 5G," *ZTE Communications*, vol. 14, no. 4, pp. 26-34, Oct. 2016.

[10] M. I. Miller and D. R. Fuhrmann, "Maximum-likelihood narrow-band direction finding and the EM algorithm," *IEEE Trans. Acoust., Speech, Sign. Process.*, vol. 38, Sep. 1990.

[11] M. Pincus, "A closed form solution for certain programming problems," *Oper. Research*, pp. 690-694, 1962.

[12] S. Affes and P. Mermelstein, "Adaptive space-time processing for wireless CDMA," *in Adaptive Signal Processing: Application to Real-World Problems*, Springer, Berlin, Jan. 2003.